Generalized Buffer-State-Based Relay Selection With Collaborative Beamforming

Ryota Nakai, *Student Member, IEEE*, Miharu Oiwa, *Student Member, IEEE*, Kyungchun Lee, *Senior Member, IEEE*, and Shinya Sugiura, *Senior Member, IEEE*

***Abstract*—In this paper, we propose a generalized buffer-state-based relaying protocol in the context of finite buffer-aided cooperative systems. The proposed relaying scheme relies on two concepts: the simultaneous activation of multiple source-to-relay links and buffer-state-based relay selection for packet transmission and reception. In order to avoid buffer overflow, as well as an empty buffer at the relay nodes, we introduce a novel thresholding scheme that gives priority to link selection. The proposed scheme is capable of achieving a lower outage probability and a lower end-to-end packet delay than existing buffer-aided relaying protocols. Moreover, the concept of collaborative beamforming is invoked for the proposed buffer-aided relaying scheme, in order to improve the received signal-to-noise ratio at the destination node. We also derive analytical bounds of the outage probability and the average packet delay of the proposed scheme with the aid of Markov-chain analysis. Our simulation results demonstrate the clear performance advantages of the proposed scheme over conventional schemes, which are especially explicit for scenarios with a high number of relay nodes.**

***Index Terms*—Broadcast, buffer, collaborative beamforming, conjugate beamforming, cooperative diversity, delay analysis, outage analysis, threshold.**

I. Introduction

RECENT buffer-aided cooperative schemes [1]–[6] have the potential to attain higher communication reliability than classic relaying schemes [7]–[9]. The use of buffers at relay nodes enables flexible scheduling of packet reception and transmission during each packet interval, resulting in a lower outage probability.[1] However, these benefits are achieved at the cost of additional overhead as well as an increased average end-to-end packet delay [3]. In [12], the max-max relay selection (MMRS) scheme was proposed in the context of a two-hop buffer-aided cooperative system, where the selections of a source-to-relay (SR) link and a relay-to-destination (RD) link are pre-scheduled, while allowing a source packet to be stored at the relay nodes until it is relayed to the destination node. Another popular buffer-aided technique is the max-link protocol [13], which was designed for selecting the single strongest available link at each time slot. The max-link protocol is capable of achieving a higher diversity gain and a better outage probability than its MMRS counterpart [12]. However, the end-to-end packet delay of the max-link protocol is typically higher than that of the MMRS protocol for the practical scenario of finite source-packet transmissions. Most recently, in order to exploit the benefits of both the MMRS and the max-link protocol, a hybrid scheme was proposed in [14], in which two-stage link selection is used in order to attain a low overhead, a low packet delay, and a low outage probability.

Inspired by the max-link protocol [13], Luo and Teh [15] proposed a sophisticated buffer-state-based (BSB) relay selection protocol for finite-buffer-aided cooperative networks that is capable of achieving a lower average packet delay than the max-link protocol [13]. This benefit is achieved because link selection is executed based on the buffer states, so that buffer overflow and an empty buffer are avoided. Furthermore, in [3] the concept of the simultaneous use of multiple SR links was introduced for the first time in the context of buffer-aided relaying protocols in order to provide additional design degrees of freedom. The protocol of [3] is capable of attaining explicit benefits in terms of end-to-end communication delay. Although noticeable benefits are attainable in the above-mentioned buffer-aided protocols [3], [15], packet delay in the buffer-aided relaying scheme is still higher than in the classic cooperative scheme, which does not rely on relay buffers, and this remains an open issue. Note that, despite its increased design degree of freedom, the protocol of [3] fails to attain a better outage performance than the conventional max-link protocol. This is because link

Manuscript received April 13, 2017; revised June 27, 2017 and September 3, 2017; accepted September 10, 2017. Date of publication September 15, 2017; date of current version February 12, 2018. This work was supported in part by the Japan Society for the Promotion of Science (JSPS) KAKENHI under Grant 26709028, Grant 17H03259, and Grant 16KK0120, and in part by the Japan–Korea Basic Scientific Cooperation Program of JSPS and the National Research Foundation (NRF) of Korea under Grant NRF-2016K2A9A2A08003700. The review of this paper was coordinated by Prof. Y. L. Guan. This paper was presented in part at the 85th IEEE Vehicular Technology Conference, Sydney, NSW, Australia, June 2017. *(Corresponding author: Shinya Sugiura.)*

R. Nakai, M. Oiwa, and S. Sugiura are with the Department of Computer and Information Sciences, Tokyo University of Agriculture and Technology, Koganei 184-8588, Japan (e-mail: rnakai@st.go.tuat.ac.jp; iwao.12394@gmail.com; sugiura@ieee.org).

K. Lee is with the Department of Electrical and Information Engineering, Seoul National University of Science and Technology, Seoul 01811, South Korea (e-mail: kclee@seoultech.ac.kr).

Color versions of one or more of the figures in this paper are available online at http://ieeexplore.ieee.org.

Digital Object Identifier 10.1109/TVT.2017.2751582

[1] In the context of general multihop networks, opportunistic routing (OR) [10], [11] has been developed for enhancing the system's throughput, by exploiting the broadcast nature of the wireless medium while assuming that all transmissions are overheard by multiple nodes. Motivated by these multihop OR algorithms, recent buffer-aided cooperative systems [1]–[6] have focused on practical two-hop wireless scenarios, while providing an analytical framework.

selection is carried out irrespective of the buffer states of the relay nodes, which prevents the potential of the protocol from being fully achieved.

Moreover, in the context of classic cooperative systems, which do not rely on relay buffers, the concept of collaborative transmit beamforming [16]–[18] was proposed as a means of improving the received signal-to-noise ratio (SNR) at the destination node. In this scheme, the distributed nodes coherently transmit a specific symbol to the destination node, by assuming that the distributed nodes are synchronized with each other, while the symbol is shared among the distributed nodes for coherent transmission. To the best of our knowledge, collaborative beamforming has not been exploited in the context of the buffer-aided relaying scenario. This is mainly because most of the previous buffer-aided relaying schemes were designed for selecting a single link per time slot, and hence packets are not shared among the relay nodes, as mentioned above.

Against this background, the novel contribution of the present paper is as follows.[2]

1) Motivated by the recent generalized max-link protocol [3], we herein propose a fixed-rate generalized buffer-aided cooperative scheme that combines two concepts: simultaneous SR link activations and BSB relay selection. The proposed protocol enables us to achieve better outage and packet-delay performances than existing buffer-aided relaying protocols, such as the max-link [13], BSB [15], and generalized max-link protocols [3].
2) Specifically, the proposed scheme is designed to allow multiple relay nodes to receive and buffer the same packet transmitted from a source node, and hence multiple copies of the transmitted packet are used to attain a diversity gain in the relaying phase. The above-mentioned limitation imposed on the generalized max-link scheme [3] is combated by introducing the principle of BSB relay selection [15]. In order to further reduce average packet delay, we incorporate a thresholding scheme that gives priority to link selection so that the number of packets stored at the relay nodes is maintained at a low rate, while at the same time avoiding empty buffers.
3) In order to further improve the achievable performance, we also incorporate the concept of collaborative beamforming into the proposed relaying scheme. This becomes realistic owing to the explicit benefits of the multiple SR-link activation. Since a packet must be shared among the collaborative relays in advance of beamforming, this benefit is specific to the proposed scheme that allows copies of a source packet in the relay buffers. In addition, the conjugate beamforming algorithm is used for the sake of maintaining the overhead as low as possible, while attaining the high beamforming gain.
4) Moreover, we derive analytical bounds of the outage probability and the average packet delay, which are valid for both the proposed scheme with collaborative beamforming and that without collaborative beamforming, by assuming infinite packet transmission. Comparison of the analytical and numerical results confirms the benefits of the proposed scheme.

The remainder of the present paper is organized as follows. In Section II, we present a system model of the proposed buffer-aided cooperative scheme. In Section III, the concept of collaborative beamforming is introduced into our buffer-aided relaying scheme. In Section IV, we derive analytical bounds of the outage probability and the average packet delay of the proposed scheme. We then provide the obtained performance results in Section V and conclude the paper in Section VI.

II. System Model

Fig. 1(a) illustrates a two-hop relaying network consisting of a single source node, K relay nodes, and a single destination node, where the kth relay node has a buffer of finite size L, while the number of packets stored at the kth relay node is represented by Ψ_k $(0 \leq \Psi_k \leq L)$. We assume that no direct link exists between the source and destination nodes and that all of the nodes operate in half-duplex mode under a decode-and-forward principle. This means that at least two time slots are required for each end-to-end packet transmission. The transmission rate of each node is maintained at r_0 bps/Hz. Moreover, we assume that there are stable low-rate feedback links and that acknowledge (ACK) packets are sent from the destination node to the relay nodes. In order to enable the ACK mechanism in this context, the size of an ACK packet is typically much smaller than a data packet; hence, a low overhead is imposed through a narrow-bandwidth channel. Alternatively, it is also possible for an ACK packet to be sent in a piggy-back manner, since control packets are periodically transmitted between the destination (coordinating) node and the relay nodes.

The rates of the kth SR and RD links are given by:

$$\mathcal{C}(h_{\mathrm{SR}_k}) = \frac{1}{2}\log_2\left(1+\gamma_{\mathrm{SR}}\left|h_{\mathrm{SR}_k}\right|^2\right), \tag{1}$$

$$\mathcal{C}(h_{\mathrm{RD}_k}) = \frac{1}{2}\log_2\left(1+\gamma_{\mathrm{RD}}\left|h_{\mathrm{RD}_k}\right|^2\right), \tag{2}$$

where h_{SR_k} and h_{RD_k} represent the associated channel coefficients, while γ_{SR} and γ_{RD} are the average SNRs of the SR and RD links, respectively. Note that since in the present paper we consider the exploitation of the half-duplex relay nodes, a prelog factor of $1/2$ is imposed on the capacity expressions of (1) and (2).[3] Throughout the present paper, we assume independent and identically distributed (IID) frequency-flat Rayleigh fading channels for all links. When the rate associated with the link of interest is higher than the transmission rate r_0, the transmitted packet is successfully decoded at the receiving node. This is a realistic assumption when considering the use of a capacity-achieving channel coding scheme, such as turbo [25] or low-density parity-check codes [26]. In contrast, when the rate is

[2]The proposed scheme was originally introduced in our preliminary work [19], which did not demonstrate the theoretical analysis, the detailed performance comparisons, or the reliability-versus-delay tradeoff specific to the proposed schemes. An additional novel contribution is that we introduce the concept of collaborative beamforming into our buffer-aided relaying scheme.

[3]The extension of the proposed scheme to that operating in the full-duplex scenario [20]–[24] is an open issue left for future studies.

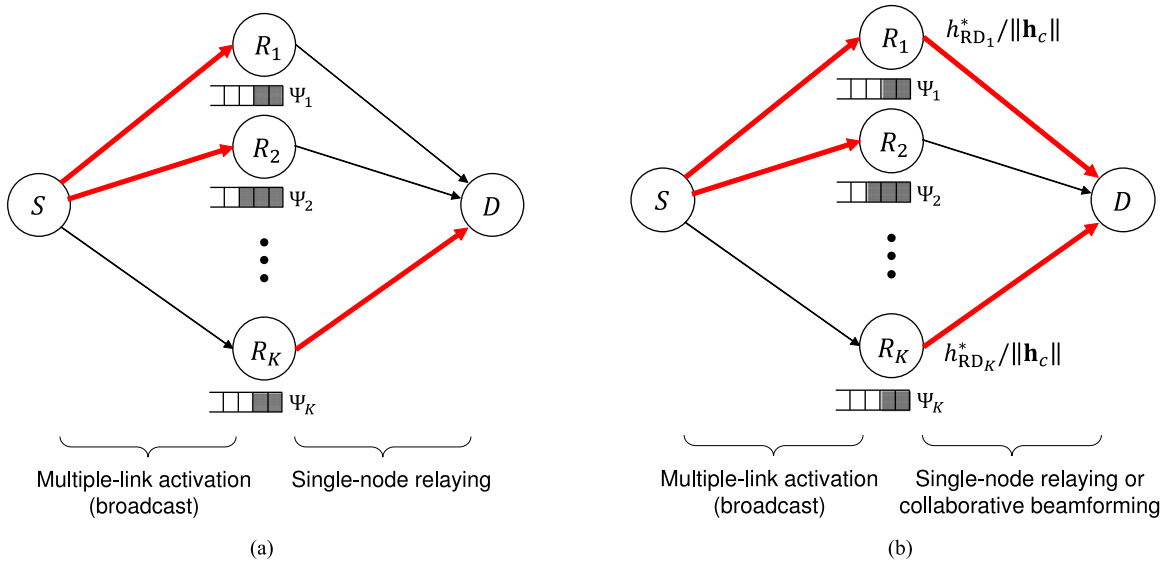

Fig. 1. System model of the proposed two-hop buffer-aided cooperative scheme, exploiting multiple SR links: (a) scheme without collaborative beamforming and (b) scheme with collaborative beamforming.

lower than the target transmission rate, the associated link experiences an outage. Thus, the outage probabilities of the local kth SR and RD links are represented by $P_{\mathrm{out}}^{\mathrm{SR}_k} = \Pr\left[\mathcal{C}(h_{\mathrm{SR}_k}) < r_0\right]$ and $P_{\mathrm{out}}^{\mathrm{RD}_k} = \Pr\left[\mathcal{C}(h_{\mathrm{RD}_k}) < r_0\right]$, respectively. In the present paper, we focus on the fixed-rate-transmission scenario [3], [12]–[15], [27], [28], rather than the adaptive-rate counterpart [29].

During each packet interval, either a source node or a relay node transmits a packet, which corresponds to the broadcast phase or the relaying phase, respectively. Furthermore, during the broadcast phase, multiple relay nodes may decode a packet owing to the broadcast nature of the wireless communications, while during relay, only a destination node decodes a packet. Note that this simultaneous use of multiple SR links in the broadcast phase has only been exploited in [3].

A. Proposed Generalized Buffer-State-Based Relaying Protocol

Similar to the protocol of [15], we use BSB relay selections in the proposed scheme, while simultaneous activation of multiple SR links is introduced at the same time. The buffer states of the relay nodes, as well as the channel coefficients of all the SR and RD links, are periodically collected at a central coordinator.[4] More specifically, both the source and relay nodes are required to transmit pilot signals to the relay and destination nodes, for the sake of allowing the channel estimation at the associated receiving nodes. Also, the channel coefficients estimated at the relay nodes have to be sent to the destination (central) node. Moreover, the central coordinator has to update the channel coefficients every channel-coherence time, while the relay nodes' buffer states have to be updated in each time slot [3]. Let us define the number of available SR and RD links, which are not in outage, by N_{SR} and N_{RD} ($0 \leq N_{\mathrm{SR}}, N_{\mathrm{RD}} \leq K$), respectively.

[4]In most of the previous studies [3], [12]–[14], [27], it was typically assumed that the destination node acts as a central coordinator in charge of link selection.

TABLE I
PRIORITY CLASSIFICATIONS OF AVAILABLE SR AND RD LINKS

Priority	Low	High	Highest
SR links	$\Psi_k = L-1$	$1 < \Psi_k < L-1$	$\Psi_k = 0, 1$
RD links	$\Psi_k = 1$	$1 < \Psi_k < \xi$	$\Psi_k \geq \xi$

After collection of the buffer states of the relay nodes, the central coordinator activates a single SR link, multiple SR links, or a single RD link, where the proposed criterion is given as follows. First, depending on the buffer states, the central coordinator evaluates the priority of each link according to Table I. More specifically, the N_{SR} available SR links are classified into three categories: low-, high-, and highest-priority SR links. The number of SR links having low, high, and the highest priorities are $N_{\mathrm{SR}}^{\mathrm{low}}$, $N_{\mathrm{SR}}^{\mathrm{high}}$, and $N_{\mathrm{SR}}^{\mathrm{highest}}$, respectively, where we have the relationship $N_{\mathrm{SR}} = N_{\mathrm{SR}}^{\mathrm{low}} + N_{\mathrm{SR}}^{\mathrm{high}} + N_{\mathrm{SR}}^{\mathrm{highest}}$. Here, the priority of the kth SR link is low when the number of packets stored at the associated relay buffer is $\Psi_k = L-1$, while the priority is high for $1 < \Psi_k < L-1$. Furthermore, the priority of the SR links is the highest when the number of stored packets is $\Psi_k = 0$ or 1. Note that when the priority of an SR link is low, the buffer state of the associated relay node is close to full, which is undesirable in terms of the maximum number of available links.

Similarly, the available N_{RD} RD links that are not in outage are categorized as low-, high-, and highest-priority RD links, where the number of links of each category is denoted by $N_{\mathrm{RD}}^{\mathrm{low}}$, $N_{\mathrm{RD}}^{\mathrm{high}}$, and $N_{\mathrm{RD}}^{\mathrm{highest}}$, respectively. Here, let us introduce an additional thresholding parameter $\xi\ (< L)$. Then, based on the buffer states of the relay nodes, the priority of the available RD links is classified as shown in Table I. When the buffer of a relay node is $\Psi_k = 1$, the priority of the associated RD link is low. Moreover, the priority is high for $1 < \Psi_k < \xi$ and is the highest for $\Psi_k \geq \xi$. Note that the threshold ξ is introduced in order to reduce the possibility of buffer overflow.

TABLE II
DECISION ALGORITHM FOR LINK ACTIVATION OF THE PROPOSED SCHEME WITHOUT COLLABORATIVE BEAMFORMING

	$N_{\mathrm{SR}}^{\mathrm{low}}$	$N_{\mathrm{SR}}^{\mathrm{high}}$	$N_{\mathrm{SR}}^{\mathrm{highest}}$	$N_{\mathrm{RD}}^{\mathrm{low}}$	$N_{\mathrm{RD}}^{\mathrm{high}}$	$N_{\mathrm{RD}}^{\mathrm{highest}}$	Decision
Case 1	—	—	≥ 1	—	—	—	Activate $N_{\mathrm{SR}}^{\mathrm{highest}} + N_{\mathrm{SR}}^{\mathrm{high}}$ highest- and high-priority SR links
Case 2	—	—	0	—	—	≥ 1	Activate a single highest-priority RD link
Case 3	—	≥ 1	0	—	—	0	Activate $N_{\mathrm{SR}}^{\mathrm{high}}$ high-priority SR links
Case 4	—	0	0	—	≥ 1	0	Activate a single high-priority RD link
Case 5	—	0	0	≥ 1	0	0	Activate a single low-priority RD link
Case 6	≥ 1	0	0	0	0	0	Activate a single low-priority SR link
Case 7	0	0	0	0	0	0	No link activated (outage event)

Having attained the priority of the available SR and RD links, link activation is carried out according to the decision classification algorithm shown in Table II. The decisions are categorized into Cases 1–7. When there is at least one highest-priority SR link, which corresponds to Case 1, all of the $N_{\mathrm{SR}}^{\mathrm{highest}} + N_{\mathrm{SR}}^{\mathrm{high}}$ highest- and high-priority SR links are activated, at which point a source packet is copied at all buffers of associated relay nodes. In Case 2, in which there is no highest-priority SR link and there is at least one highest-priority RD link, a single highest-priority RD link is activated. After the destination node successfully decodes the packet relayed from the selected relay node, the destination node transmits an ACK packet to all of the relay nodes via the stable feedback channels, and the corresponding packet copied at the relay nodes is deleted from the buffers. Furthermore, when there are high-priority SR links and when there are no highest-priority SR and RD links, which corresponds to Case 3, all of the $N_{\mathrm{SR}}^{\mathrm{high}}$ high-priority SR links are activated. In Case 4, there are high-priority RD links but no highest-priority SR, highest-priority RD, or high-priority SR links, and a single strongest high-priority RD link is activated. In Cases 5 and 6, we have only low-priority SR and RD links, where the decisions are the same as those of Cases 4 and 3, respectively, except that the high-priority links are replaced by low-priority links. Finally, Case 7 corresponds to an outage event, because there are no available links.[5]

In order to provide further insight, there are other benefits specific to the proposed decision algorithm shown in Table II. More specifically, in the proposed algorithm, when there are several RD candidate links that have the same priority level, the link associated with the highest channel amplitude is selected, as in Cases 2, 3, 6, and 7 of Table II. This allows us to achieve two benefits. First, from a practical point of view, channel estimation must be carried out at each receive node, although, for the sake of simplicity, we herein assume the acquisition of perfect channel state information. Hence, by choosing the link with the highest channel amplitude, the effects of potential channel estimation errors may be reduced. Another benefit is that the transmit power may be reduced at each transmit node. More specifically, by assuming the use of powerful near-capacity channel coding schemes, an infinitesimally low error-rate performance is attainable if the transmission rate is lower than $\mathcal{C}$ in (1) and (2). Hence, as long as $R < \mathcal{C}$ is satisfied, the transmission power can be reduced, and this power-reduction effect is the highest when we choose the link with the highest channel coefficient. This benefit is especially explicit when the relay nodes are mobile terminals, which are power-limited.[6]

TABLE III
LEGITIMATE BUFFER STATES OF $K = 2$ RELAY NODES WITH $(L = 2)$-SIZED BUFFERS

States	Relay 1		Relay 2	
s_1	empty	empty	empty	empty
s_2	◯	empty	empty	empty
s_3	empty	empty	◯	empty
s_4	◯	□	empty	empty
s_5	◯	empty	□	empty
s_6	empty	empty	◯	□
s_7	◯	△	□	empty
s_8	◯	empty	□	△
s_9	◯	△	□	◊
s_{10}	◯	empty	◯	empty
s_{11}	◯	△	◯	empty
s_{12}	◯	empty	◯	△
s_{13}	◯	△	◯	△
s_{14}	◯	△	◯	□
s_{15}	◯	empty	□	◯
s_{16}	◯	△	□	◯
s_{17}	□	◯	◯	empty
s_{18}	□	◯	◯	△
s_{19}	□	◯	△	◯

B. Example of Buffer States for $K = 2$ and $L = 2$

As an example, let us consider the specific scenario of $K = 2$ relay nodes, each employing an $(L = 2)$-sized buffer. Similar to the generalized max-link scheme [3], all of the buffer states are shown in Table III. Here, the $K = 2$ relay nodes are allowed to share a specific packet. Note that the four symbols shown in Table III, i.e., ◯, △, □, and △, denote four different packets. The total number of states is $N_{\mathrm{state}} = 19$. Specifically, the first

[5]In the present paper, we focus on the max-link-based protocol, where the conventional max-link protocol [13] is improved by relying on simultaneous SR-link activation as well as BSB link selection. However, the concept presented herein is readily applicable to the MMRS-based protocol [12], [30] that pre-schedules the SR and RD link selection. In such a scheme, the average packet delay and overhead required for updating the channel and buffer states may be reduced in comparison to the max-link counterpart, which is achieved at the cost of increased outage probability, similar to [3].

[6]To be more specific, such a link-level adaptive-power transmission between a transmitter and a receiver is carried out, after a specific link is selected by a central coordinator, similar to the conventional adaptive-rate buffer-aided relay selection [29].

nine states s_i $(i = 1, \cdots, 9)$ correspond to those considered in the conventional max-link and BSB schemes, where a specific packet is not shared at the $K = 2$ relay nodes. In the remaining ten states s_i $(i = 10, \cdots, 19)$, copies of the source packets at different relay nodes are allowed.

Fig. 2(a) and (b) show the state diagrams of the Markov model of the conventional generalized max-link protocol and the proposed protocol without collaborative beamforming, respectively, where each of the $K = 2$ relay nodes has a buffer of $L = 2$. Note again that, in the generalized max-link scheme [3], which is the extended version of the max-link scheme [13], multiple SR-link activation is enabled, while no restrictions are imposed on the buffer states. Since both the conventional generalized max-link and the proposed protocol allow the relay nodes to share copies of a specific source packet, the number of legitimate states in both cases is $N_{\text{state}} = 19$.

As shown in Fig. 2(a), in the conventional generalized max-link protocol, all 19 states are reachable from any state. In contrast, since in the proposed protocol, empty- and full-buffer states are restricted, according to our decision algorithm (shown in Table II), six states, namely, s_{13}, s_{15}, s_{16}, s_{17}, s_{18}, and s_{19}, are not reachable under the assumption that the initial state is given by empty-buffer state s_1. This is because the proposed scheme is designed for imposing a limitation on the link selection algorithm, in order to avoid empty- and full-buffer states, which tend to reduce the maximum attainable diversity order. In contrast, in the conventional generalized max-link scheme, these undesirable states are reached by the transitions, as indicated by the blue dotted arrows in Fig. 2(a).

In order to clarify the above-mentioned transitions of the proposed scheme, let us consider the transition from state s_{10}, in which a single packet is shared between the two relay nodes. Transitions from state s_{10} are only possible to states s_1, s_{11}, and s_{12}, as shown in Fig. 2(b). More specifically, the transition from state s_{10} to state s_1 occurs when either of the two RD links is activated. Then, when the destination node successfully receives the packet, an ACK packet is sent back to both relay nodes, which allows deletion of the associated packet from the relay buffers. As for the transition from state s_{10} to state s_{11} or state s_{12}, either of the two SR links is activated, since simultaneous activation of the two SR links is avoided, according to Case 6 of our algorithm, as shown in Table II.

In order provide further insights, let us exemplify the case where the first SR link is in outage. More specifically, we consider the state where each of the two relay nodes stores a single different packet, which corresponds to state s_5. Then, since the first SR link is in outage, the number of packets stored at the buffer of the first relay node remains unchanged or decreases in the next link selection event. Hence, as shown in the state diagram of Fig. 2(b), the possible transitions from state s_5 are to states s_2 (the second RD link selection), s_3 (the first RD link selection), s_5 (the outage event), and s_8 (the second SR link selection).

C. Effects of Thresholding Parameter ξ

In the proposed protocol, the thresholding parameter ξ must be designed in advance of link selections. By appropriately setting the threshold ξ, we can characterize the performance tradeoff between outage probability and average packet delay. Note that a low ξ value tends to maintain the number of packets stored in the buffers to be low, which has a beneficial effect on end-to-end packet delay, since the average packet delay is directly related to the number of stored packets, as formulated later in Section IV-B. In contrast, this reduction in the number of stored packets may reduce the number of available RD links in following transitions, potentially resulting in an increased outage probability.

In our extensive simulations, we found that a low ξ value tends to result in a low average packet delay and a slightly higher outage probability. However, for the scenario of a high number of relay nodes, the effect of the increased outage probability was marginal, owing to a sufficiently high number of available links, as will be clarified in Section V-D. Hence, in the remainder of the present paper, we maintain the thresholding parameter at $\xi = 2$ in order to achieve a low packet delay.[7]

III. Proposed Scheme With Collaborative Beamforming

In our generalized BSB relaying scheme (proposed in Section II-A), the multiple SR links are simultaneously exploited in the broadcast phase, while only a single RD link is used in the relaying phase. In this section, we introduce the concept of collaborative transmit beamforming into our relaying scheme, in order to allow simultaneous exploitation of the multiple RD links in the relaying phase.

In conventional buffer-aided relaying schemes, which do not rely on the simultaneous activation of multiple SR links, the incorporation of collaborative beamforming is not realistic. This is because only a single relay node is activated in each time slot, and so no specific source packet is shared among the relay nodes. In contrast, as described in Section II-A, the proposed scheme is designed for sharing a source packet among the relay nodes, which allows us to readily use collaborative beamforming in the proposed scheme, as shown in Fig. 1(b).

More specifically, the proposed scheme is characterized by operating with collaborative beamforming as follows. Similar to the scheme proposed in Section II-A, the priority of each SR and RD link is evaluated by a central coordinator, according to Table I. Then, the type of link activation is decided from among the four modes, i.e., activation of a single SR link, activation of a single RD link, activation of multiple SR links, or activation of multiple RD links, according to the algorithm shown in Table IV. Note that the activation of multiple RD links corresponds to collaborative beamforming. More specifically, when a relay node stores a packet that is ready for transmission, which is shared with other relay nodes, the packet may be transmitted in a collaborative manner from all of the relay nodes that share the packet, rather than simply being transmitted from a single relay node. Similar to the proposed scheme without collaborative beamforming, the decisions are categorized into Cases 1–7,

[7]Note that, for the proposed scheme using collaborative beamforming, the use of $\xi = 3$ resulted in a slightly lower packet delay compared to the use of $\xi = 2$. However, for the sake of simplicity, we used $\xi = 2$ as a basic parameter in both of the proposed schemes.

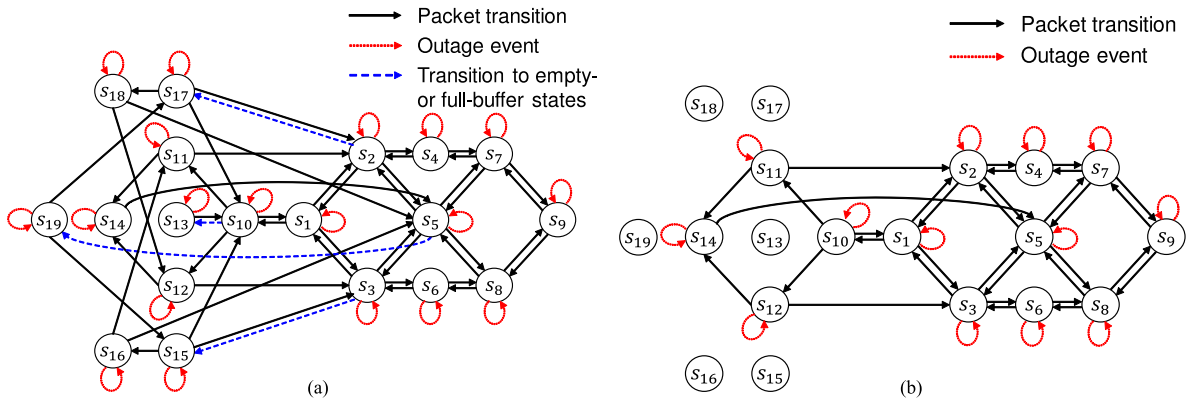

Fig. 2. State diagram of the Markov chain model representing (a) the conventional generalized max-link scheme and (b) the proposed scheme without collaborative beamforming with $K = 2$ relay nodes and a buffer size of $L = 2$.

TABLE IV
DECISION ALGORITHM FOR LINK ACTIVATION OF THE PROPOSED SCHEME WITH COLLABORATIVE BEAMFORMING

	$N_{\mathrm{SR}}^{\mathrm{low}}$	$N_{\mathrm{SR}}^{\mathrm{high}}$	$N_{\mathrm{SR}}^{\mathrm{highest}}$	$N_{\mathrm{RD}}^{\mathrm{low}}$	$N_{\mathrm{RD}}^{\mathrm{high}}$	$N_{\mathrm{RD}}^{\mathrm{highest}}$	Decision
Case 1	—	—	≥ 1	—	—	—	Activate $N_{\mathrm{SR}}^{\mathrm{highest}} + N_{\mathrm{SR}}^{\mathrm{high}}$ highest- and high-priority SR links
Case 2	—	—	0	—	—	≥ 1	Activate $N_{\mathrm{RD}}^{\mathrm{highest}}$ highest-priority RD links (collaborative beamforming)
Case 3	—	≥ 1	0	—	—	0	Activate $N_{\mathrm{SR}}^{\mathrm{high}}$ high-priority SR links
Case 4	—	0	0	—	≥ 1	0	Activate $N_{\mathrm{RD}}^{\mathrm{high}}$ high-priority RD links (collaborative beamforming)
Case 5	—	0	0	≥ 1	0	0	Activate $N_{\mathrm{RD}}^{\mathrm{low}}$ low-priority RD links (collaborative beamforming)
Case 6	≥ 1	0	0	0	0	0	Activate a single low-priority SR link
Case 7	0	0	0	0	0	0	No link activated (outage event)

where only the difference is that, in the proposed scheme with collaborative beamforming, Cases 2, 4, and 5 are replaced by multiple RD-link activation.

Here, let us consider the RD channels associated with the collaborative relay nodes as $\mathbf{h}_c = [h_c^{(1)}, \cdots, h_c^{(Q)}]^T$ for a specific state, where Q is the number of the collaborative relay nodes. According to the selection of the central coordinator, the collaborative relay nodes may simultaneously transmit the shared packet, where a normalized conjugate channel coefficient of $h_c^{(q)*}/\|\mathbf{h}_c\|$ is multiplied by the symbol at the qth collaborative relay node before the transmission. Here, the normalization factor maintains the total instantaneous transmit power of the collaborative relay nodes to be constant. Hence, the associated rate is formulated as

$$\mathcal{C}_c = \frac{1}{2}\log_2\left(1 + \gamma_{\mathrm{RD}}\|\mathbf{h}_c\|^2\right). \tag{3}$$

This beamforming method corresponds to conjugate beamforming [31], [32], which maximizes the beamforming gain in terms of the received SNR at the destination node. As the explicit benefit of conjugate beamforming, where the weight of each node is simply given by the conjugate of a channel coefficient, the collaborations between relay nodes are significantly simplified, in comparison to other beamforming schemes.[8] However, other types of beamforming schemes are readily applicable to our buffer-aided collaborative beamforming protocol. The rule of the other link activation process is the same as that of the originally proposed process that does not use collaborative beamforming. This implies that when the capacity associated with the collaborative beamforming (3) is lower than capacity of a single strongest RD link, the latter tends be activated.

In order to further elaborate, let us consider the special scenarios of $(K, L) = (2, 2)$ considered in Table III.[9] Among the total $N_{\mathrm{state}} = 19$ states, collaborative beamforming may be carried out by the transition from states $s_{10}, s_{11}, s_{12}, s_{13}, s_{14}, s_{15}, s_{16}, s_{17}$, and s_{18}.[10] More specifically, for these states, we simply have the RD channels associated with collaborative beamforming as $\mathbf{h}_c = [h_c^{(1)}, h_c^{(2)}]^T = [h_{\mathrm{RD}_1}, h_{\mathrm{RD}_2}]^T$.

Naturally, this collaborative beamforming scheme is capable of achieving a better outage probability, which is imposed by the cost of the additional overhead required for synchronizing the collaborative relay nodes.

[8]However, the unignorable synchronization cost still exists, even in the proposed buffer-aided conjugate-beamforming-based scheme. Hence, either of the two proposed schemes with/without collaborative beamforming may be selected in an appropriate manner, depending on the requirement of the overhead-reliability tradeoff.

[9]The state diagram of the proposed collaborative beamforming scheme is equivalent to that without collaborative beamforming, which is shown in Fig. 2(b). This is because, in the proposed scheme, which does not rely on collaborative beamforming, the packet copies stored at the relay nodes are deleted after ACK receptions from the destination node.

[10]Note that collaborative beamforming can never be carried out by the transition from state s_{19}, since the packets that are ready for transmission at the two relay nodes, i.e., packets □ and △, are not shared.

The proposed scheme relying on collaborative beamforming is expressed as a Markov model, similar to that dispensing with collaborative beamforming, shown in Fig. 2(b). Hence, the analytical framework derived in Section IV is readily applicable to both schemes with and without collaborative beamforming.

IV. Theoretical Bounds

In this section, we analyze the outage probability and the average packet delay of the proposed scheme. Here, we take into account the effects of finite-size buffers at relay nodes. Moreover, similar to conventional analysis, we assume that a sufficiently large number of packets are transmitted from the source node to the destination node [13], [14]. For simplicity, we focus on a specific scenario of $K = 2$ relay nodes with $(L = 2)$-sized buffers, which corresponds to the states listed in Table III. However, our analytical framework is readily applicable to that supporting arbitrary system parameters (K, L). Note that the two proposed schemes are designed to allow a specific source packet to be stored at buffers of different relay nodes, although in most of the conventional buffer-aided protocols, such as max-link and BSB protocols, a source packet is stored only at a single selected relay node. This increases the number of legitimate states associated with the Markov model on the proposed scheme.

A. Outage-Probability Analysis

We introduce a Markov chain model that is valid specifically for the proposed scheme. As shown in Table III, we have a total of $N_{\text{state}} = 19$ states.

We denote by Ξ_n and Ξ_n^a the set of legitimate links and the set of available links, respectively, for state s_n. Thus, we have the relationship $\Xi_n^a \subset \Xi_n$. Furthermore, we consider that U_n is the set of states that have the possibility of being arrived from state s_n through a one-step transition. Here, let us define $\mathbf{A} \in \mathbb{R}^{N_{\text{state}} \times N_{\text{state}}}$ as the transition matrix of the Markov model of Fig. 2(b). Then, the element in the ith row and jth column of $\mathbf{A}$ is represented as [15]

$$\mathrm{A}_{ij} = \sum_{\Xi_j^a \subset \Xi_j} \Pr(\Xi_j^a) \Pr(s_j \rightarrow s_i | \Xi_j^a), \tag{4}$$

where $s_i \in U_j$ is a state that is directly connected to the state s_j. Moreover, $\Pr(\Xi_j^a)$ of (4) corresponds to the probability that a subset of links Ξ_j^a of the legitimate set Ξ_j can successfully convey a packet without an outage, which is expressed by [15]

$$\begin{aligned} \Pr(\Xi_j^a) = & \prod_{h_{\mathrm{SR}_k} \in \Xi_j^a} (1 - P_{\text{out}}^{\mathrm{SR}_k}) \prod_{h_{\mathrm{SR}_k} \in \Xi_j, h_{\mathrm{SR}_k} \notin \Xi_j^a} P_{\text{out}}^{\mathrm{SR}_k} \\ & \prod_{h_{\mathrm{RD}_k} \in \Xi_j^a} (1 - P_{\text{out}}^{\mathrm{RD}_k}) \prod_{h_{\mathrm{RD}_k} \in \Xi_j, h_{\mathrm{RD}_k} \notin \Xi_j^a} P_{\text{out}}^{\mathrm{RD}_k}, \end{aligned} \tag{5}$$

where $P_{\text{out}}^{\mathrm{SR}_k}$ is the outage probability of the kth SR link, and $P_{\text{out}}^{\mathrm{RD}_k}$ is that of the kth RD link. More specifically, the outage probabilities of the SR and RD links are formulated by $P_{\text{out}}^{\mathrm{SR}_k} = 1 - \exp(-(2^{2R} - 1)/\gamma_{\mathrm{SR}})$ and $P_{\text{out}}^{\mathrm{RD}_k} = 1 - \exp(-(2^{2R} - 1)/\gamma_{\mathrm{RD}})$, respectively [3].

The steady-state probabilities $\boldsymbol{\pi} \in \mathbb{R}^{N_{\text{state}}}$ are formulated in closed-form as [3]

$$\boldsymbol{\pi} = (\mathbf{A} - \mathbf{I} + \mathbf{B})^{-1} \mathbf{b} \in \mathbb{R}^{N_{\text{state}}}. \tag{6}$$

The theoretical outage-probability bound is formulated as [13]

$$P_{\text{out}} = \mathrm{diag}(\mathbf{A}) \boldsymbol{\pi}. \tag{7}$$

B. Average Packet Delay

In this section, we present the average packet-delay bound of the proposed protocol. In a manner similar to that of previous studies [14], [27], we assume infinite source-packet transmissions and finite-buffer relay nodes.

Based on Little's law [27], the average packet delay induced at the kth relay node is represented by

$$\mathbb{E}[T_k] = \frac{\mathbb{E}[\Psi_k]}{\eta_k}, \tag{8}$$

where η_k denotes the average throughput of the kth relay node. Considering that the probabilities of selecting any of the relay nodes are identical, as mentioned in [27], the average packet delay of each relay node is expressed as (8).

Specifically, (8) is given by

$$\mathbb{E}[T_k] = \frac{2}{1 - P_{\text{out}}} \sum_{i=1}^{N_{\text{state}}} \pi_i \Psi(i), \tag{9}$$

where π_i represents the ith element of the state vector $\boldsymbol{\pi}$, and $\Psi(i)$ is the number of different packets stored at the K relay nodes for state π_i. Here, $\mathbb{E}[\cdot]$ represents the expectation operation. Moreover, $p_{kj}(i)$ denotes the probability that the jth RD link is selected and that a packet stored at the kth relay node decreases.

V. Performance Results

In this section, we present our simulation results in order to characterize the proposed protocol and compare it with existing schemes. For simplicity, the transmission rate r_0 of each node was maintained to be $r_0 = 1$ bps/Hz. The buffers at all of the relay nodes were set to empty in the initial condition, and a sufficiently large number of packets were transmitted from the source node to the destination node in each Monte Carlo simulation.[11] All of the SR and RD channels are randomly generated at each time slot. The max-link protocol [13], the generalized max-link protocol [3], and the BSB protocol [15] were chosen as benchmark schemes. The basic system parameters used in our simulations are listed in Table V. Whereas in Sections V-A–D, we considered the symmetric-channel scenarios of $\gamma = \gamma_{\mathrm{SR}} = \gamma_{\mathrm{RD}}$, in Section V-E, we assumed asymmetric channels, i.e., $\gamma_{\mathrm{SR}} \neq \gamma_{\mathrm{RD}}$.

[11] More specifically, in our simulations, more than $N_p = 10^5$ packets were generated for calculating each numerical curve. As shown later in Fig. 3, the numerical curves coincided with the analytical curve, which was derived under the assumption of an infinite number of packets. Furthermore, our extensive simulations confirmed that when we varied the number of packets per frame from $N_p = 10^2$ to 10^7, $N_p = 10^5$ packets per frame were sufficient in terms of convergence, which was unaffected by the initial states.

TABLE V
PARAMETERS USED IN THE SIMULATIONS

Channel	IID frequency-flat Rayleigh fading
– Symmetric	$\gamma = \gamma_{SR} = \gamma_{RD}$
– Asymmetric	$\gamma_{SR} \neq \gamma_{RD}$
Number of relay nodes K	2 – 30
Buffer size L	2 – 30
Thresholding value ξ	$2 \leq \xi \leq L$
Average SNR value	0–30 dB
Number of packets per frame N_p	10^5

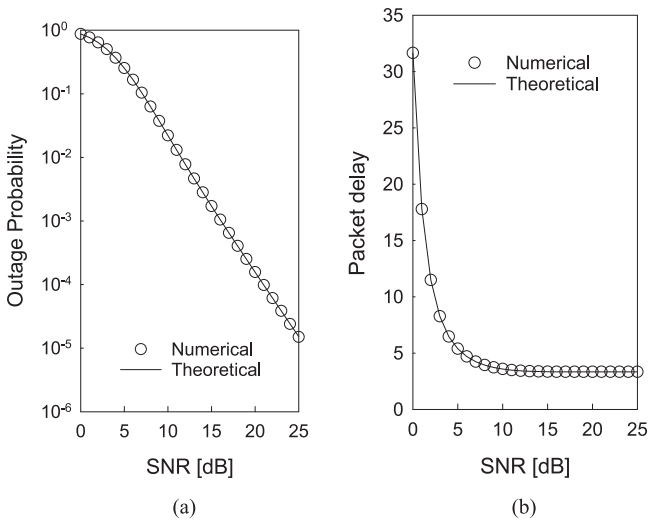

Fig. 3. Analytical and numerical results of the proposed scheme without collaborative beamforming, where we varied SNR from 0 dB to 25 dB, and the number of relay nodes was set to $K = 2$, each with buffer size $L = 2$. Moreover, infinite source-packet transmissions were assumed. (a) Outage probability, and (b) packet delay.

A. Comparisons of Theoretical and Numerical Results

In order to validate our numerical results, we compared the analytical and numerical results. Specifically, we examined the outage probability and the packet delay of the proposed scheme without collaborative beamforming and with $K = 2$ relay nodes, each with an ($L = 2$)-sized buffer in Fig. 3(a) and (b), respectively. As shown in Fig. 3(a) and (b), the analytical and numerical curves agreed well for each metric. Note that while Fig. 3 theoretically verifies the performance of the proposed scheme without collaborative beamforming in terms of outage probability and delay profile, that of the proposed scheme with collaborative beamforming was also validated in our simulations, where the theoretical and numerical curves coincided (similar to Fig. 3).

B. Packet-Delay Performance

Fig. 4(a)–(c) show the average number of different packets stored in the K relay nodes for the proposed scheme, the max-link scheme [13], the generalized max-link scheme [3], and the BSB scheme [15], where we considered the parameters $(K, L) = (3, 5)$, $(5, 5)$, and $(5, 10)$. The SNR was varied from 0 dB to 25 dB with a step of 5 dB, while the number of transmitted packets per Monte Carlo simulation was set to $N_p = 10^5$. For each (K, L) scenario, the proposed scheme without collaborative beamforming exhibited the lowest number of stored packets among the five schemes, whereas the proposed scheme with collaborative beamforming attained the second-best performance. More specifically, the gap between the two proposed schemes and the three benchmark schemes increased with increasing SNR. Note that the number of packets stored in the relay nodes is directly related to the analytical packet delay, as seen in the numerator of (8). This implies that the proposed scheme tends to exhibit the lowest packet delay profile. In addition, the proposed scheme is characterized by multiple copies of a specific source packet existing in the buffers of the relay nodes. This contributes to the reduction of the average number of different packets, in comparison to the max-link and BSB schemes.[12]

Next, Fig. 5 shows the average packet-delay profiles of the proposed scheme, the max-link scheme [13], the generalized max-link scheme [3], and the BSB scheme [15], where the buffer size L was set to $L = 10$, while varying the number of relay nodes from $K = 2$ to 10. The average SNR was $\gamma = 5$ and 15 dB in Fig. 5(a) and (b), respectively. Observe in Fig. 5 that the proposed scheme without collaborative beamforming achieved the lowest packet delay among the five schemes considered herein, where the delay remained nearly unchanged, regardless of the number of relay nodes. In contrast, in the max-link and BSB schemes, the packet delay increased upon increasing the number of relay nodes. This implies that the advantage of the proposed scheme is more explicit, especially for a scenario involving a large number of relay nodes. Moreover, the beneficial effects of the proposed scheme became explicit at high SNRs.

In Fig. 6, we also compared the packet delay of the five schemes, where $K = 5$ relay nodes were considered, while varying the buffer size from $L = 4$ to 20. The average SNR was maintained to be $\gamma = 10$ dB. Similar to Fig. 5, the proposed scheme without collaborative beamforming exhibited the best packet delay profile over the entire range of L. More specifically, the packet delay of the two proposed schemes remained constant, irrespective of the value of L. This is because our thresholding scheme maintained the number of packets stored at the relay nodes to be low and so contributed to the reduction of packet delay, as expected from the analytical bound of (9).

C. Outage-Probability Performance

Having investigated the packet-delay profile of the proposed scheme, let us now examine its reliability. Since the empty- and full-buffer states tend to reduce the number of available links, i.e., the spatial diversity gain, the packet distributions

[12] In order to provide further insights, the number of different packets stored at the relay nodes increases, upon increasing the buffer size L or the number of relay nodes K. Hence, higher values of K or L may increase packet delay, despite the improved outage-probability performance.

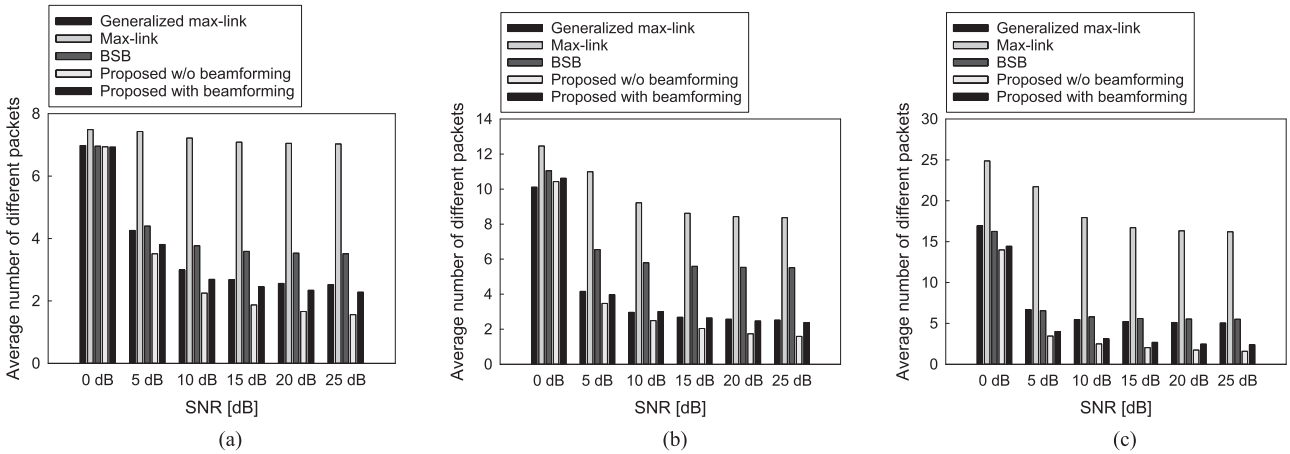

Fig. 4. Average number of different packets stored at the relay nodes, where the parameters were given by $(K, L) = (3, 5), (5, 5)$, and $(5, 10)$, and the SNR was varied from 0 to 25 dB with a step of 5 dB. (a) $(K, L) = (3, 5)$. (b) $(K, L) = (5, 5)$. (c) $(K, L) = (5, 10)$.

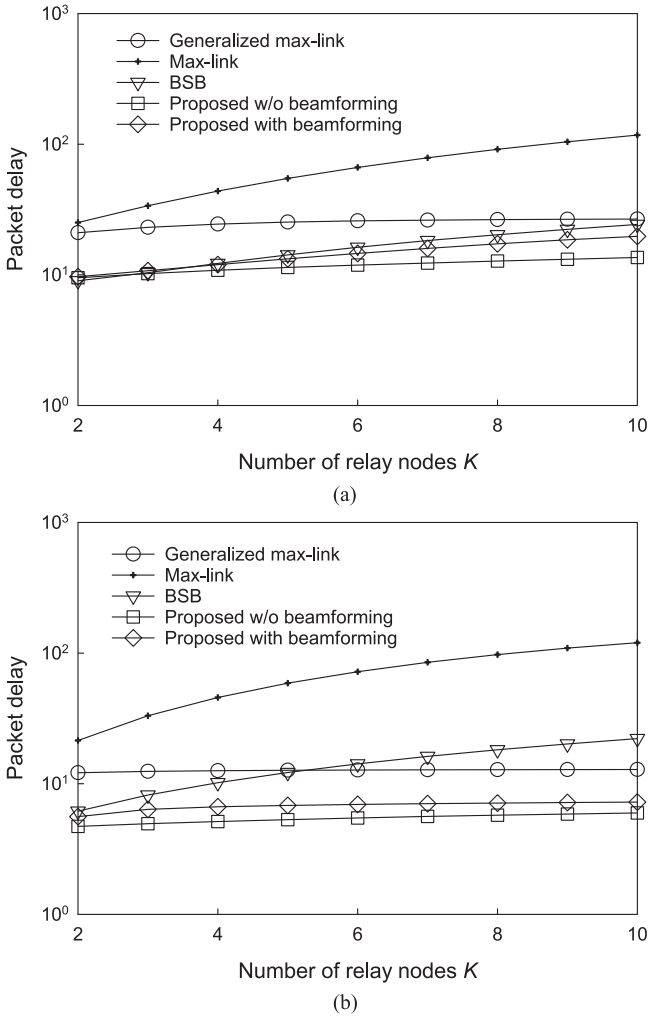

Fig. 5. Average packet-delay of the proposed scheme, the max-link scheme [13], the generalized max-link scheme [3], and the BSB scheme [15], where the buffer size was set to $L = 10$, while varying the number of relay nodes from $K = 2$ to 10. (a) $\gamma = 5$ dB. (b) $\gamma = 15$ dB.

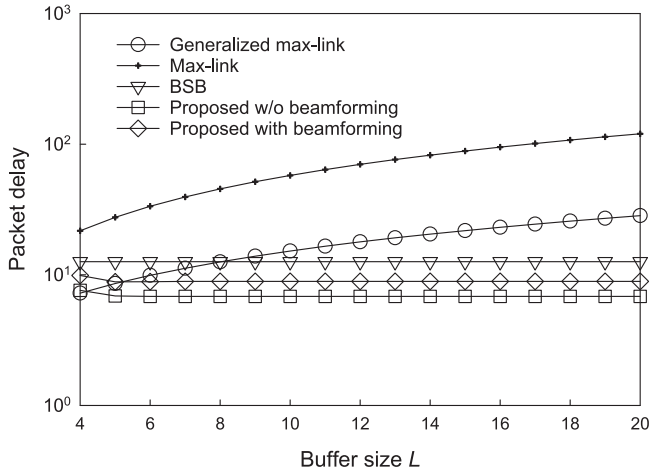

Fig. 6. Average packet-delay of the proposed, max-link scheme [13], the generalized max-link scheme [3], and the BSB scheme [15], where we considered $K = 5$ relay nodes, while varying the buffer size from $L = 4$ to 20. The average SNR was maintained to be $\gamma = 10$ dB.

in the relay buffers are closely related to the outage performance.

In order to clarify these effects, Table VI lists the distributions of buffer states in the simulations over 10^5 time slots for $K = 3$ relay nodes, each having an $(L = 5)$-sized buffer, at SNR $=$ 10 dB and 20 dB. In each SNR scenario, the proposed and BSB schemes successfully avoided the empty- and full-buffer states, which was achieved as the explicit benefit of the buffer-state-based link selections. This allows us to maintain the attainable diversity order to be nearly maximum. In contrast, the generalized max-link and max-link schemes suffered from a reduction in the number of available links, where for each SNR scenario, the relay buffers are either empty or full during more than 20% of the transmission interval.

Next, Fig. 7 shows the effects of the number of relay nodes on the outage probability for the five schemes, where the system parameters are the same as those used in Fig. 5, in which the

TABLE VI
DISTRIBUTIONS OF BUFFER STATES IN THE SIMULATIONS OVER 10^5 TIME SLOTS FOR $K = 3$ RELAY NODES WITH ($L = 5$)-SIZED BUFFERS

Number of stored packets	0	1	2	3	4	5
Generalized max-link (SNR = 10 dB)	10.4%	18.7%	20.7%	20.7%	18.5%	11.0%
Max-link (SNR = 10 dB)	10.8%	16.3%	17.5%	18.6%	19.9%	16.9%
BSB (SNR = 10 dB)	0.4%	73.8%	25.4%	0.4%	0.0%	0.0%
Proposed w/o beamforming ($\xi = 2$, SNR = 10 dB)	1.6%	31.6%	47.3%	16.8%	2.7%	0.2%
Proposed with beamforming ($\xi = 2$, SNR = 10 dB)	1.0%	29.4%	44.3%	20.1%	5.2%	0.0%
Generalized max-link (SNR = 20 dB)	9.9%	19.6%	20.1%	20.3%	19.8%	10.3%
Max-link (SNR = 20 dB)	9.3%	15.6%	17.3%	19.0%	20.9%	17.9%
BSB (SNR = 20 dB)	0.0%	82.3%	17.7%	0.0%	0.0%	0.0%
Proposed w/o beamforming ($\xi = 2$, SNR = 20 dB)	0.0%	44.0%	50.1%	5.9%	0.0%	0.0%
Proposed with beamforming ($\xi = 2$, SNR = 20 dB)	0.0%	25.5%	48.2%	24.2%	2.1%	0.0%

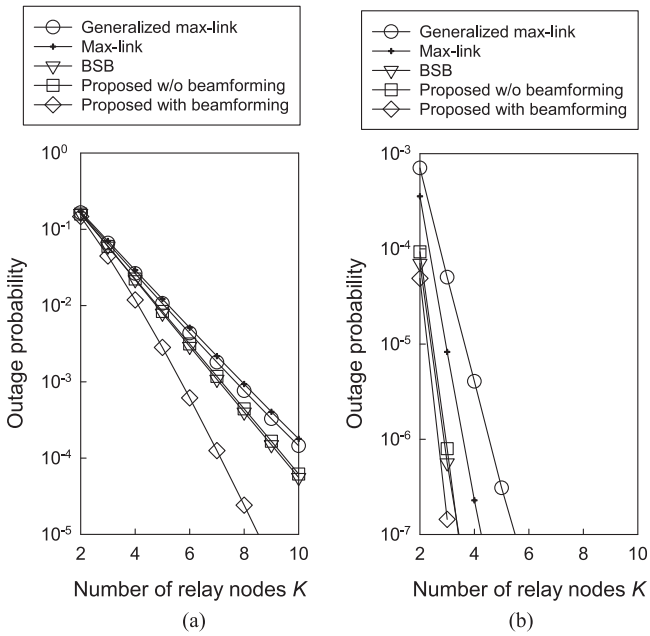

Fig. 7. Outage probabilities of the proposed scheme, the max-link scheme [13], the generalized max-link scheme [3], and the BSB scheme [15], where the buffer size was $L = 10$, while the number of relay nodes was varied from $K = 2$ to 10. (a) $\gamma = 5$ dB. (b) $\gamma = 15$ dB.

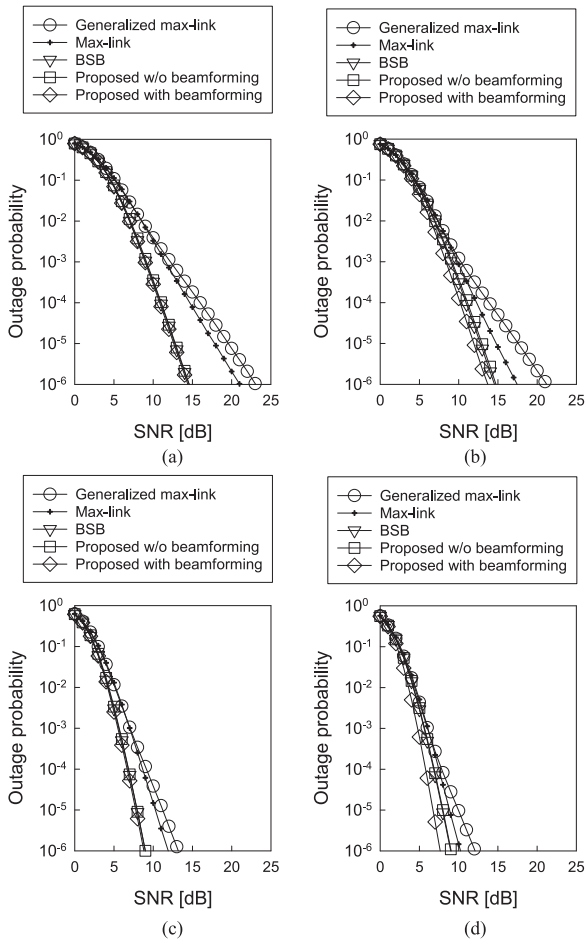

Fig. 8. Outage probabilities of the proposed scheme, the max-link scheme [13], the generalized max-link scheme [3], and the BSB scheme [15]. (a) $(K, L) = (3, 3)$. (b) $(K, L) = (3, 10)$. (c) $(K, L) = (6, 3)$. (d) $(K, L) = (6, 10)$.

average SNR was $\gamma = 5$ dB in Fig. 7(a) and 15 dB Fig. 7(b). As shown in Fig. 7, all of the schemes improved the outage performance upon increasing the number of relay nodes. The proposed scheme with collaborative beamforming exhibited the best outage probability performance, followed by the proposed scheme without collaborative beamforming and the BSB scheme, as expected from the results shown in Table VI. This is achieved by the explicit benefits of the collaborative beamforming gain, as well as the maximum attainable diversity gain owing to the absence of empty- and full-buffer states, which is particularly noticeable for a high-K scenario.

In addition, Fig. 8 compares the effects of the SNR on the outage probability, where the system parameters were $(K, L) = (3, 3), (3, 10), (6, 3)$, and $(6, 10)$ in Fig. 8(a)–(d), respectively. For the $L = 3$ scenarios shown in Fig. 8(b) and (c), the two proposed schemes exhibited approximately the same performance as that of the BSB scheme, where the performance advantage over the max-link and generalized max-link schemes increased upon increasing the SNR value, owing to the high maximum attainable diversity gain. In Fig. 8(b) and (d), where the buffer size was increased to $L = 10$, the proposed scheme with collaborative beamforming had an explicit advantage over the BSB scheme and the proposed scheme without collaborative beamforming.

In order to explicitly show the tradeoff between the packet delay and the outage probability in each scheme, in Fig. 9, we plotted the delay with respect to the outage probability,

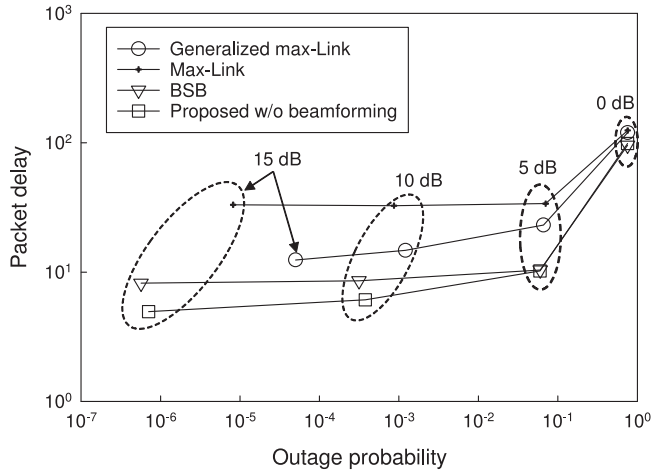

Fig. 9. Packet delay and outage probability of the proposed scheme, the max-link scheme [13], the generalized max-link scheme [3], and the BSB scheme [15], where we considered $K = 3$ relay nodes, each with a buffer size of $L = 10$. The average SNR was varied from $\gamma = 0$ to 15 dB.

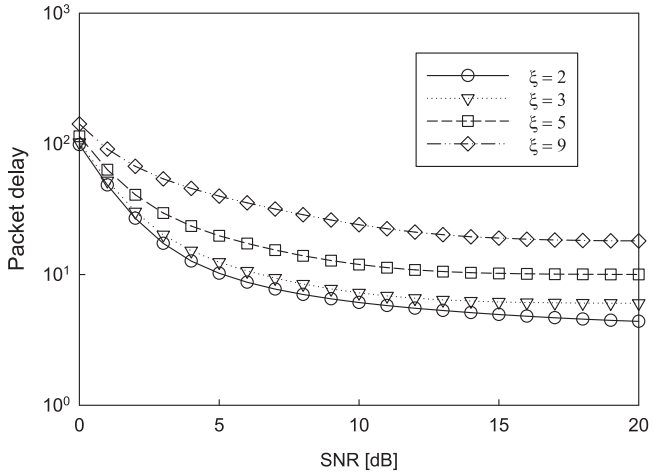

Fig. 10. Average packet-delay comparisons of the proposed scheme without collaborative beamforming, where the parameters of the relay nodes were $(K, L) = (3, 10)$, while the thresholding parameter was varied from $\xi = 2$ to 9.

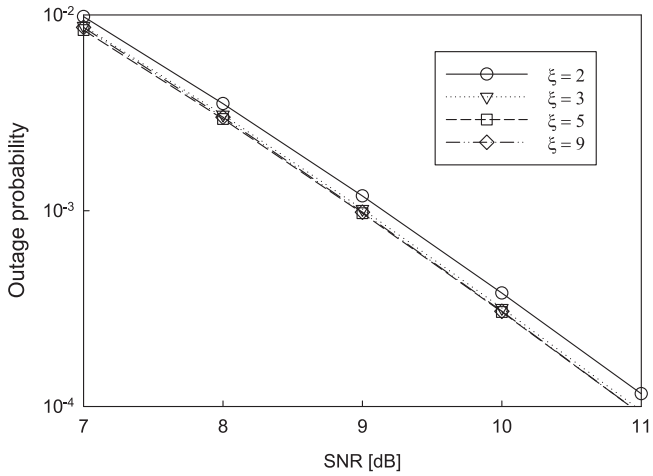

Fig. 11. Outage probability of the proposed scheme without collaborative beamforming, where the parameters of the relay nodes were $(K, L) = (3, 10)$, while the thresholding parameter was varied from $\xi = 2$ to 9.

where we considered $K = 3$ relay nodes, each with a buffer size of $L = 10$. The average SNR was varied from $\gamma = 0$ to 15 dB. Observe in Fig. 9 that upon increasing the SNR value, the outage probability and the packet delay improved for all four schemes. More specifically, the proposed scheme exhibited the lowest packet delay, where the advantage increased with the increase in the SNR value, while the best outage performances were achieved by the proposed scheme and the BSB scheme and were similar for these schemes.

D. Effects of Parameter ξ

Next, the effects of the thresholding parameter, ξ, were investigated. In the above simulations, ξ was fixed to two, since it typically provides nearly the best packet-delay performance, while maintaining good outage performance, comparable to that of the BSB scheme. However, by appropriately determining parameter ξ, the proposed scheme is capable of striking a balance between reliability and packet delay. In order to demonstrate these characteristics, Figs. 10 and 11 show the effects of parameter ξ on the performance of the packet delay and the outage probability, respectively, where the parameters of the relay nodes are $(K, L) = (3, 10)$, while varying the thresholding parameter from $\xi = 2$ to 9. As shown in Fig. 10, the average packet delay improved as the thresholding parameter ξ, decreased, where the best performance was achieved by $\xi = 2$, as expected. In contrast, as shown in Fig. 11, an increase in ξ slightly improved the performance of the outage probability, where the maximum performance gap between the curve of $\xi = 2$ and that of $\xi = 9$ was as low as 0.2 dB. This implies that, although a performance tradeoff exists between the packet delay and the outage probability, it may be beneficial to use $\xi = 2$ for the sake of carrying out low-packet-delay operation, while attaining a good outage probability.

In order to further elaborate, as shown in Fig. 12, we investigated the effects of parameter ξ on the achievable performance of the proposed scheme without collaborative beamforming for

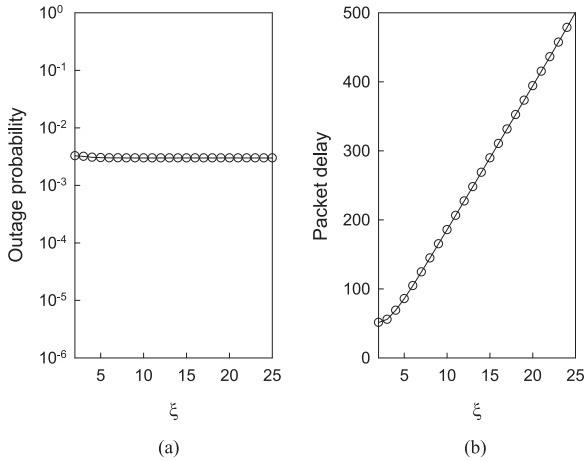

Fig. 12. Effects of parameter ξ on the achievable performance of the proposed scheme without collaborative beamforming, where the system parameters were $(K, L) = (30, 30)$ and the SNR was 1 dB. Parameter ξ was varied from 2 to 30. (a) Outage probability, and (b) packet delay.

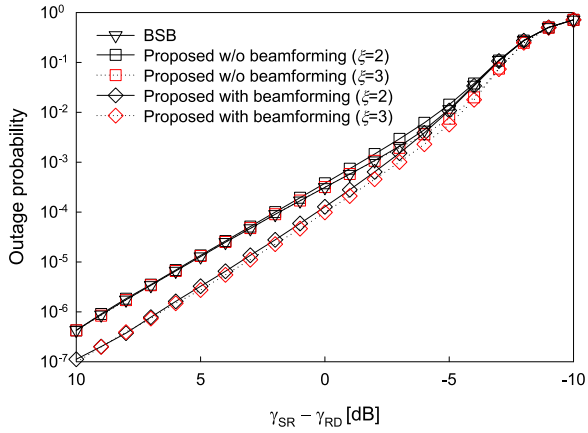

Fig. 13. Outage-probabilities of the proposed scheme with and without collaborative beamforming in the asymmetric channels, where the parameters of the relay nodes were $(K, L) = (3, 10)$, while the thresholding parameter was set to $\xi = 2$ and 3. The average SNR of the RD links was maintained to be $\gamma_{\mathrm{RD}} = 10$ dB.

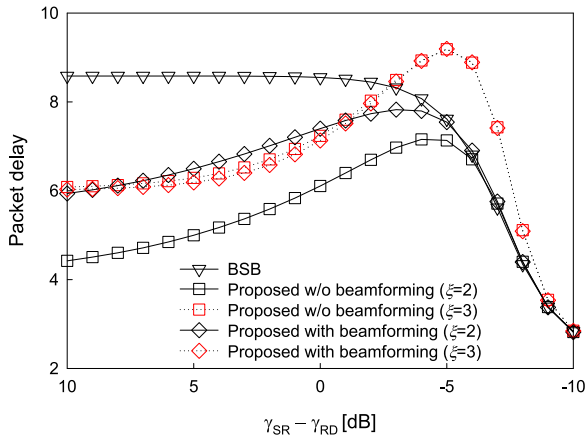

Fig. 14. Average packet-delays of the proposed scheme with and without collaborative beamforming in the asymmetric channels, where the parameters of the relay nodes were $(K, L) = (3, 10)$, while the thresholding parameter was set to $\xi = 2$ and 3. The average SNR of the RD links was maintained to be $\gamma_{\mathrm{RD}} = 10$ dB.

a high-scale $(K, L) = (30, 30)$ scenario. Here, the SNR was 1 dB, while parameter ξ was varied from 2 to 30. More specifically, Fig. 12(a) and (b) show the outage probability and the packet delay, respectively. As shown in Fig. 12, $\xi = 2$ yielded the lowest packet delay, while achieving a good outage probability performance, as expected. Hence, the design guideline remained unchanged even for the scenario involving high values of K and L.

E. Effects of Asymmetric Channels

Finally, in this section, we consider the scenarios of the asymmetric channels, i.e., $\gamma_{\mathrm{SR}} \neq \gamma_{\mathrm{RD}}$. Figs. 13 and 14 show the outage-probability and packet-delay for the proposed scheme with and without collaborative beamforming, respectively. The parameters of the relay nodes were $(K, L) = (3, 10)$, while the thresholding parameter was set to $\xi = 2$ and 3. The average SNR of the RD links was maintained to be $\gamma_{\mathrm{RD}} = 10$ dB. The BSB scheme was chosen as the benchmark scheme, because this scheme was designed for achieving better performance in both symmetric- and asymmetric-channel scenarios compared to other existing schemes, as mentioned in [15]. As shown in Figs. 13 and 14, the proposed scheme with collaborative beamforming achieved the best outage probability performance, while the proposed scheme without collaborative beamforming attained a better packet delay profile (similar to symmetric-channel scenarios) than the other schemes.

Furthermore, the results of Fig. 14 ensure the basic trends of the proposed schemes. For example, the proposed scheme without collaborative beamforming, having a lower ξ value, results in a lower packet delay, while the packet delay of the proposed scheme without collaborative beamforming tends to be lower than that of the proposed scheme relying on collaborative beamforming. However, an exceptional trend was also seen in Fig. 14, where in the proposed collaborative beamforming scheme, the packet delay of the $\xi = 2$ scenario was not explicitly lower than that of $\xi = 3$. This is mainly because a packet, which is stored at only a single relay node, tends to remain in the buffer, since a packet shared among multiple relay nodes is more likely to be transmitted via collaborative beamforming in our algorithm of Table IV. This detrimental effect in terms of the packet delay is, more explicit in the $\xi = 2$ scenario, than in the $\xi = 3$ one.

VI. Conclusion

In the present paper, we proposed a novel buffer-aided cooperative scheme, which, for the first time, exploits the concepts of simultaneous activation of multiple SR links and BSB link selections. The clear benefits of the proposed scheme are better outage and packet-delay performance compared to existing fixed-rate buffer-aided cooperative schemes. In order to further improve the outage probability performance, we incorporated the concept of collaborative beamforming into the proposed scheme, which enables the simultaneous use of multiple RD links, in addition to SR links. We also derived the outage-probability and packet-delay bounds of the proposed scheme. Numerical investigations confirmed the benefits of the proposed scheme over the existing schemes, while clarifying that the performance tradeoff between reliability and delay can be adjusted by adjusting the thresholding parameter, ξ.

References

[1] B. Xia, Y. Fan, J. Thompson, and H. V. Poor, "Buffering in a three-node relay network," *IEEE Trans. Wireless Commun.*, vol. 7, no. 11, pp. 4492–4496, Nov. 2008.

[2] C. Dong, L. L. Yang, and L. Hanzo, "Multi-hop diversity aided multi-hop communications: A cumulative distribution function aware approach," *IEEE Trans. Commun.*, vol. 61, no. 11, pp. 4486–4499, Nov. 2013.

[3] M. Oiwa and S. Sugiura, "Reduced-packet-delay generalized buffer-aided relaying protocol: Simultaneous activation of multiple source-to-relay links," *IEEE Access*, vol. 4, pp. 3632–3646, 2016.

[4] N. Nomikos *et al.*, "A survey on buffer-aided relay selection," *IEEE Commun. Surveys Tuts.*, vol. 18, no. 2, pp. 1073–1097, Apr.–Jun. 2016.

[5] J. Hajipour, A. Mohamed, and V. C. M. Leung, "Channel-, queue-, and delay-aware resource allocation in buffer-aided relay-enhanced OFDMA networks," *IEEE Trans. Veh. Technol.*, vol. 65, no. 4, pp. 2397–2412, Apr. 2016.

[6] R. Simoni, V. Jamali, N. Zlatanov, R. Schober, L. Pierucci, and R. Fantacci, "Buffer-aided diamond relay network with block fading and inter-relay interference," *IEEE Trans. Wireless Commun.*, vol. 15, no. 11, pp. 7357–7372, Nov. 2016.

[7] J. N. Laneman, D. N. C. Tse, and G. W. Wornell, "Cooperative diversity in wireless networks: Efficient protocols and outage behavior," *IEEE Trans. Inf. Theory*, vol. 50, no. 12, pp. 3062–3080, Dec. 2004.
[8] G. Kramer, M. Gastpar, and P. Gupta, "Cooperative strategies and capacity theorems for relay networks," *IEEE Trans. Inf. Theory*, vol. 51, no. 9, pp. 3037–3063, Sep. 2005.
[9] B. Rankov and A. Wittneben, "Spectral efficient protocols for half-duplex fading relay channels," *IEEE J. Sel. Areas Commun.*, vol. 25, no. 2, pp. 379–389, Feb. 2007.
[10] S. Biswas and R. Morris, "Opportunistic routing in multi-hop wireless networks," *ACM SIGCOMM Comput. Commun. Rev.*, vol. 34, no. 1, pp. 69–74, 2004.
[11] H. Liu, B. Zhang, H. T. Mouftah, X. Shen, and J. Ma, "Opportunistic routing for wireless ad hoc and sensor networks: Present and future directions," *IEEE Commun. Mag.*, vol. 47, no. 12, pp. 103–109, Dec. 2009.
[12] A. Ikhlef, D. S. Michalopoulos, and R. Schober, "Max-max relay selection for relays with buffers," *IEEE Trans. Wireless Commun.*, vol. 11, no. 3, pp. 1124–1135, Mar. 2012.
[13] I. Krikidis, T. Charalambous, and J. S. Thompson, "Buffer-aided relay selection for cooperative diversity systems without delay constraints," *IEEE Trans. Wireless Commun.*, vol. 11, no. 5, pp. 1957–1967, May 2012.
[14] M. Oiwa, C. Tosa, and S. Sugiura, "Theoretical analysis of hybrid buffer-aided cooperative protocol based on max–max and max–link relay selections," *IEEE Trans. Veh. Technol.*, vol. 65, no. 11, pp. 9236–9246, Nov. 2016.
[15] S. Luo and K. Teh, "Buffer state based relay selection for buffer-aided cooperative relaying systems," *IEEE Trans. Wireless Commun.*, vol. 14, no. 10, pp. 5430–5439, Oct. 2015.
[16] H. Ochiai, P. Mitran, H. V. Poor, and V. Tarokh, "Collaborative beamforming for distributed wireless ad hoc sensor networks," *IEEE Trans. Signal Process.*, vol. 53, no. 11, pp. 4110–4124, Nov. 2005.
[17] V. Havary-Nassab, S. Shahbazpanahi, A. Grami, and Z. Q. Luo, "Distributed beamforming for relay networks based on second-order statistics of the channel state information," *IEEE Trans. Signal Process.*, vol. 56, no. 9, pp. 4306–4316, Sep. 2008.
[18] R. Mudumbai, D. R. B. Iii, U. Madhow, and H. V. Poor, "Distributed transmit beamforming: Challenges and recent progress," *IEEE Commun. Mag.*, vol. 47, no. 2, pp. 102–110, Feb. 2009.
[19] R. Nakai, M. Oiwa, and S. Sugiura, "Generalized buffer-state-based relay selection for fixed-rate buffer-aided cooperative systems," in *Proc. IEEE 85th Veh. Technol. Conf.*, Sydney, NSW, Australia, Jun. 4–7, 2017, pp. 1–5.
[20] A. Ikhlef, J. Kim, and R. Schober, "Mimicking full-duplex relaying using half-duplex relays with buffers," *IEEE Trans. Veh. Technol.*, vol. 61, no. 7, pp. 3025–3037, Sep. 2012.
[21] S. N. Hong and G. Caire, "Virtual full-duplex relaying with half-duplex relays," *IEEE Trans. Inf. Theory*, vol. 61, no. 9, pp. 4700–4720, Sep. 2015.
[22] S. M. Kim and M. Bengtsson, "Virtual full-duplex buffer-aided relaying in the presence of inter-relay interference," *IEEE Trans. Wireless Commun.*, vol. 15, no. 4, pp. 2966–2980, Apr. 2016.
[23] K. T. Phan and T. Le-Ngoc, "Power allocation for buffer-aided full-duplex relaying with imperfect self-interference cancelation and statistical delay constraint," *IEEE Access*, vol. 4, pp. 3961–3974, 2016.
[24] D. Qiao, "Effective capacity of buffer-aided full-duplex relay systems with selection relaying," *IEEE Trans. Commun.*, vol. 64, no. 1, pp. 117–129, Jan. 2016.
[25] S. Sugiura, S. Chen, and L. Hanzo, "MIMO-aided near-capacity turbo transceivers: Taxonomy and performance versus complexity," *IEEE Commun. Surveys Tuts.*, vol. 14, no. 2, pp. 421–442, May 2012.
[26] N. Bonello, S. Chen, and L. Hanzo, "Low-density parity-check codes and their rateless relatives," *IEEE Commun. Surveys Tuts.*, vol. 13, no. 1, pp. 3–26, Feb. 2011.
[27] Z. Tian, G. Chen, Y. Gong, Z. Chen, and J. Chambers, "Buffer-aided max-link relay selection in amplify-and-forward cooperative networks," *IEEE Trans. Veh. Technol.*, vol. 64, no. 2, pp. 553–565, Feb. 2015.
[28] N. Zlatanov and R. Schober, "Buffer-aided relaying with adaptive link selection—fixed and mixed rate transmission," *IEEE Trans. Inf. Theory*, vol. 59, no. 5, pp. 2816–2840, May 2013.
[29] I. Ahmed, A. Ikhlef, R. Schober, and R. K. Mallik, "Power allocation for conventional and buffer-aided link adaptive relaying systems with energy harvesting nodes," *IEEE Trans. Wireless Commun.*, vol. 13, no. 3, pp. 1182–1195, Mar. 2014.
[30] P. K. Upadhyay and P. K. Sharma, "Max-max user-relay selection scheme in multiuser and multirelay hybrid satellite-terrestrial relay systems," *IEEE Commun. Lett.*, vol. 20, no. 2, pp. 268–271, Feb. 2016.
[31] T. L. Marzetta, "Noncooperative cellular wireless with unlimited numbers of base station antennas," *IEEE Trans. Wireless Commun.*, vol. 9, no. 11, pp. 3590–3600, Nov. 2010.
[32] H. Yang and T. L. Marzetta, "Performance of conjugate and zero-forcing beamforming in large-scale antenna systems," *IEEE J. Sel. Areas Commun.*, vol. 31, no. 2, pp. 172–179, Feb. 2013.

Ryota Nakai (S'17) was born in Shizuoka, Japan, in 1994. He received the B.E. degree in computer and information sciences from Tokyo University of Agriculture and Technology, Koganei, Japan, in 2017. He is currently working toward the Postgraduate degree in the Department of Computer and Information Sciences, Tokyo University of Agriculture and Technology. His research interests include cooperative wireless communications and physical layer security.

He received the IEEE VTS Tokyo Chapter 2017 Young Researcher's Encouragement Award.

Miharu Oiwa (S'16) was born in Tsukuba, Japan, in 1994. She received the B.E. degree in computer and information sciences from Tokyo University of Agriculture and Technology, Koganei, Japan, in 2016. She is currently working toward the Postgraduate degree in the Department of Computer and Information Sciences, Tokyo University of Agriculture and Technology. Her research interests include cooperative wireless communications and networks.

She received the IEEE VTS Tokyo Chapter 2016 Young Researcher's Encouragement Award and the 32nd Telecom System Technology Student Award (honorable mention) from the Telecommunications Advancement Foundation in 2017.

Kyungchun Lee (M'11–SM'16) received the B.S., M.S., and Ph.D. degrees in electrical engineering from the Korea Advanced Institute of Science and Technology, Daejeon, South Korea, in 2000, 2002, and 2007, respectively. From April 2007 to June 2008, he was a Postdoctoral Researcher at the University of Southampton, Southampton, U.K. From July 2008 to August 2010, he was with the Samsung Electronics, Suwon, South Korea. Since September 2010, he has been at Seoul National University of Science and Technology, Seoul, South Korea. His research interests include signal processing and optimization for wireless communications with a focus on massive MIMO, interference coordination, and cooperative systems. He received the Best Paper Award at the IEEE International Conference on Communications in 2009.

Shinya Sugiura (M'06–SM'12) received the B.S. and M.S. degrees in aeronautics and astronautics from Kyoto University, Kyoto, Japan, in 2002 and 2004, respectively, and the Ph.D. degree in electronics and electrical engineering from the University of Southampton, Southampton, U.K., in 2010.

From 2004 to 2012, he was a Research Scientist with the Toyota Central Research and Development Laboratories, Inc., Nagakute, Japan. Since 2013, he has been an Associate Professor with the Department of Computer and Information Sciences, Tokyo University of Agriculture and Technology, Koganei, Japan, where he heads the Wireless Communications Research Group. He authored or coauthored more than 50 IEEE journal papers. His research interests include wireless communications, networking, signal processing, and antenna technology.

Dr. Sugiura received a number of awards, including the Sixth RIEC Award from the Foundation for the Promotion of Electrical Communication in 2016, the Young Scientists' Prize by the Minister of Education, Culture, Sports, Science and Technology of Japan in 2016, the 14th Funai Information Technology Award (First Prize) from the Funai Foundation in 2015, the 28th Telecom System Technology Award from the Telecommunications Advancement Foundation in 2013, the Sixth IEEE Communications Society Asia–Pacific Outstanding Young Researcher Award in 2011, the 13th Ericsson Young Scientist Award in 2011, and the 2008 IEEE Antennas and Propagation Society Japan Chapter Young Engineer Award. He was also certified as an Exemplary Reviewer of IEEE COMMUNICATIONS LETTERS in 2013 and 2014.